Anonymous Referee #1

Received and published: 18 June 2018

AC = Liisa Juusola et al.,
Received and published: 26 June 2018

Using the two dimensional global hybrid-Vlasov model Vlasiator, Juusola et al studied the characteristics and source of current sheet flapping in the center of the magnetotail. Their simulations show that an initial down-tail propagating current sheet displacement caused by a hemispherically asymmetric magnetopause perturbation can launch a standing magnetosonic wave within the magnetotail, which acts as a resonance cavity, creating subsequent flapping waves in the current sheet. In three dimensional, Juusola et al suggest that such source mechanism for current sheet flapping could create kink-like waves that had been observed to emit from the center of the tail towards the dawn-dusk flanks. The simulation results from this study could potentially provide explanation on the mechanism for current sheet flapping, which till this day remains unknown, and increase our understanding of the tail flapping phenomenon. However, much clarification is needed as terminologies are not clearly defined and loosely used. Analysis of results to support their conclusion are lacking, vague and qualitative. In my opinion, major revisions to the manuscript and further clarifications are required.

AC: We thank the Referee for their constructive comments. We are happy to make many of the suggested changes. In some cases we suggest alternative approaches, in order to avoid making the manuscript too long to be concise and readable. Please see below for our point-by-point replies.

Comments: 1. Page 1 Line 19: Shouldn't it be "up and down relative to the spacecraft", instead of "back and forth across the spacecraft"? Please clarify.

AC: Yes, we are happy to make the suggested correction.

2. Page 2 Line 9: Insert appropriate reference Sun et al., [2013] THEMIS Observation of a magnetotail current sheet flapping.

AC: We can add the reference.

3. Page 2 Line 9: In this sentence, the authors categorized current sheet flapping events into three types (Steady, kink-like along y and kink-like along x). To my understanding of this study, Juusola et al focused primarily on the "kink-type along x" current sheet flapping. However, subsequently in the text, the authors used the word current sheet flapping to describe tailward propagating displacement of the current sheet, which I take it to mean "kink-type along x". However, the term current sheet flapping is more commonly described as steady or kink-like along the y-direction in current literature. The authors should clearly state or define what kind of current sheet flapping they are referring to throughout the text so as to not confuse the readers. If at all possible, I would suggest the authors to avoid using tail flapping in this study since many current sheet flapping studies using THEMIS and Cluster data concluded that the current sheet flapping waves travel towards the dawn or dusk flanks (e.g. See review paper by M. Volwerk), which to my understanding from the text, is not what the authors are referring to. This will avoid confusing the readers.

AC: As explained in the first paragraph of the Introduction (page 1, lines 17-21), the term current sheet flapping has originally been used to refer to up and down motion of the current sheet that can be observed as variations in Bx. We show that our simulated signatures produce the appropriate Bx time series, and thus using the term "current sheet flapping" should be justified.

In later studies, different types of flapping (all of which can produce similar time series of Bx) have been distinguished (page 2, lines 3-10). These include the kink-like flapping in the y direction. Because this kind of flapping has been so widely studied, as also pointed out by the Referee, we wanted to make it clear to the reader that our analysis does not directly apply to it, although the results could be relevant to it as well (page 2, lines 27-29).

In order to clarify the issue, we suggest to modify the text on page 2, lines 27-29 to: “Because the simulation is 2D, we concentrate on the characteristics and source of the waves in the center of the tail (i.e., waves in the x-z plane). We also discuss the possibility that in 3D, they could drive the kink-like waves that are emitted from the center of the tail and propagate dawnward and duskward (i.e., waves in the y-z plane).”

4. Page 3 Line 13: The authors should justify their choice of solar wind parameters in their simulation. A particular set of solar wind conditions, instead of a range of values, are used in this study. This begs the question of how does the solar wind conditions affect the simulation results and conclusion of this study.

AC: A particular set of solar wind conditions instead of a range of values was used because of the heavy computational load of running this type of a simulation. This same run has been analyzed in several previous studies as well (page 2, lines 23-25). The run was suitable for our study, because current sheet flapping occurred in it. How solar wind conditions affect the results is a very interesting question indeed. However, it is outside the scope of this study.

5. Page 3 Line 23: I strongly suggest that the authors start section 3 with the simulation results shown in Figure 7. By replacing Figure 1 with Figure 7, it will provide context for readers who are either not used to or not familiar with simulation studies and improve the flow of the manuscript.

AC: We are happy to make the suggested change.

6. Page 5 Line 10: One of the main conclusions of this simulation study was that the “asymmetric perturbation consists of a simultaneous compression of the northern tail lobe and expansion of the southern tail lobe” drives current sheet flapping as shown in their simulation results. However, it is unclear whether this asymmetric perturbation in the simulation is physical or numerical. Furthermore, the authors mentioned that this asymmetric perturbation is caused by subsolar magnetic reconnection (line 8), which is counter-intuitive. Under steady solar wind conditions and dayside reconnection occurring at the subsolar magnetopause region, shouldn’t the loading of the open flux in the two hemisphere of the tail be equal? One might think that unequal loading of open flux in the northern and southern tail lobe is caused by dayside reconnection occurring at higher latitude. Would this implies that the perturbation is a numerical effect? Furthermore, Figure 3 shows that there are regions of high beta around the nightside magnetopause surface. Are there turbulence occurring on the magnetopause surface? Could that been the cause of the asymmetric perturbation? Please clarify.

AC: Loading of open flux in the two hemispheres should indeed be equal under steady southward solar wind conditions. However, the loading process can still create hemispherically asymmetric perturbations. As shown by Hoilijoki et al. (2017) and Jarvinen et al., (2018), the perturbations created by subsolar reconnection (magnetic islands, exhaust jets, waves) in the simulation are hemispherically asymmetrical at any given moment of time. The instabilities are seeded by noise at the numerical level, which is not symmetrical. Furthermore, as pointed out by the Referee, turbulence can create and strengthen the asymmetric perturbation as well. Thus, the hemispherically asymmetric magnetopause perturbation that we interpret to initiate the flapping can, according to

our understanding, be interpreted to be of physical origin. Because we do not believe that the exact creation mechanism of the perturbation is relevant to the results (page 7, lines 17-24), we have omitted any further analysis of its creation from the text.

7. Page 6 Line 9: The use of “cross-tail direction”, which traditionally referred to the y-direction, is very confusing. The simulation is two dimensional in the x and z-direction. Unless the authors meant cross-tail in the z-direction? If that’s the case, the authors should be clear on that as ambiguous use of words could mislead the readers.

AC: We are happy to replace “cross-tail” with “x-z”.

8. Page 7 Line 1: In the discussion section, Juusola et al suggested that in three dimensions, the asymmetric perturbation could have a finite extent in the y-direction, thus driving current sheet flapping in the dawn-dusk direction. However, the authors neither substantiate their conclusion with any 3D simulations results nor conduct any experiments that investigate the effects of a finite IMF By on the occurrence and properties of tail flapping waves. Since the authors listed this as one of the five main conclusion of this study, I think substantial work should be done to demonstrate the connection between asymmetric perturbation mechanism and current sheet flapping in the dawn-dusk direction as observed by earlier studies, rather than simply providing a hand-wavy, qualitative explanation.

AC: We agree with the Referee that listing such claims as conclusions would require further analysis, and we suggest to remove the last point from the list of conclusions in section 5. However, we find these to be valid discussion points, the examination of which could lead to further studies. Thus, we would still like to mention the possibility that the flapping created through our suggested mechanism could act as a source for the waves that propagate in the y direction both in the abstract and in section 5 (as a separate paragraph below the list of conclusions). However, we would further emphasize that this is only a suggestion and would require further study. For example: “The suggested mechanism could act as a source for kink-like waves that are emitted from the center of the tail and propagate toward the dawn and dusk flanks. However, further research using a 3D simulation will be needed to examine this suggestion.” Page 1, lines 12-13 could be modified to: “It may be possible that the suggested mechanism could act as a source for kink-like waves that have been observed to be emitted from the center of the tail and to propagate toward the dawn and dusk flanks.”

9. Page 7 Line 25: Juusola et al stated model predictions for the purpose of future validations with satellite observations. However, the authors did not follow up on this idea of validations with observations, which I think is a wonderful idea. If it is the authors’ intention to validate their simulation results with observations, this study should provide more quantitative results (e.g. what is the relationship between flapping period and lobe pressure? Does it follows a power law or linear relation etc?) and measurable quantities. These information could be easily obtained from the simulation.

AC: We agree that it may be desirable to derive more quantitative predictions for the purpose of further validations with observations. However, providing numbers for the validation is not straightforward, because they are likely to depend not only on the driving solar wind conditions but the history of the magnetospheric dynamics. A simple confirmation that the period of the flapping signatures decreases as the lobe pressure increases would be a good starting point, and numbers could be provided when running several 3D simulations representing a range of solar wind conditions becomes possible, which would probably require a full dedicated study.

Anonymous Referee #1

Received and published: 26 June 2018

Dear Juusola et al.,
Thank you for your replies to my comments on the manuscript. It adequately answers my questions and concerns. I have no further questions or concerns. It is an interesting study on current sheet flapping and I look forward to reading future studies on this research topic.
Sincerely

AC: -

Anonymous Referee #2

Received and published: 23 June 2018

AC = Liisa Juusola et al.,
Received and published: 26 June 2018

Using the 2-D global hybrid-Vlasov model Vlasiator, authors studied the response of magnetotail at the tail center to the magnetopause perturbation, created by subsolar magnetopause reconnection. Authors declared that the appeared oscillation of tail Bx component should be the kink-like flapping motion propagating towards both tail flanks. Nonetheless, the simulation is 2-D, The variation of this osscillation in Y direction can't be investigated, it is still hard to convince readers that the oscillation of Bx component is indeed associated with the kink-like flapping propagating azimuthally. I will explain my reasons in the following.

AC: We thank the Referee for their comments and drawing our attention to the fact that some clarification of the text is needed: our intent was not to declare that the simulated oscillations are the kink-type wave that propagates in the dawn-dusk direction but waves in the x-z plane. It was an item of discussion that these waves could maybe act as a source for the waves that propagate in the y direction. Please see below for our detailed replies to the comments and suggested modifications to the text.

Major comment
As stated in the introduction, Rong et al.(2015) found that the different flapping modes can yield a same flapping sequence of Bx component. How can you differentiate these flapping modes in your simulation? In my view, only the 3-D simulation can unambiguously answer it.

AC: As the simulation is 2D in the x-z plane it cannot contain the kind of waves that propagate in the y direction. Rong et al. (2015) mention two kinds of waves in the x-z plane. It should be possible to analyze the normal directions of the waves to separate these, but we do not consider this to be relevant to our conclusions. We analyze the wave signatures in the x-z plane, determine a mechanism that can start and maintain these waves, and then discuss the possibility that in 3D our suggested mechanism could function in the midnight sector. We suggest that, in 3D, these waves could act as a source for the waves that are emitted from the midnight sector and propagate in the

dawn-dusk direction. In order to make this more clear, we would suggest to modify page 2, lines 27-29 to: “Because the simulation is 2D, we concentrate on the characteristics and source of the waves in the center of the tail (i.e., waves in the x-z plane). We also discuss to possibility that in 3D, they could drive the kink-like waves that are emitted from the center of the tail and propagate dawnward and duskward (i.e., waves in the y-z plane).” We have also suggested some further clarifications in the abstract and conclusions in response to the comments by Referee #1.

Specific comments

1. Line 16 of page 2, the paper of Shen et al.[2008,AG] and Forsyth et al.,(2009,AG) should be cited when referring the disturbance of solar wind flow as the flapping source. Shen, C., Z. J. Rong, X. Li, M. Dunlop, Z. X. Liu, H. V. Malova, E. Lucek, and C. Carr (2008), Magnetic configurations of tail tilted current sheet, Ann. Geophys., 26, 3525–3543. Forsyth, C., M. Lester, R. C. Fear, E. Lucek, I. Dandouras, A. N. Fazakerley, H. Singer, and T. K. Yeoman (2009), Solar wind and substorm excitation of the wavy current sheet, Ann. Geophys., 27, 2457–2474.

AC: We can add these references.

2. The joint observation of flapping event by TC-1 and Cluster (Zhang et al., 2005,AG) showed that the kink-like flapping waves propagate longitudinally with the same flapping phase at different X coordinates. However, it can not be characterized in your 2-D simulation, e.g. Fig1. Zhang, T. L., et al. (2005), Double Star/Cluster observation of neutral sheet oscillations on 5 August 2004, Ann. Geophys., 23, 2909–2914.

AC: Considering the 1 min temporal resolution and relatively small (5 RE) separation in x direction between the satellites in the study by Zhang et al. (2005), we do not see that there would be a discrepancy between our results and theirs.

3. Fig.3 predicts a dispersive flapping waves with time-increased frequency. To my knowledge, there is no observation evidence to back up it. Careful comparisons are needed.

AC: We agree with the Referee and indeed suggest further studies to validate the simulation results against observations (page 7, lines 25-26).

4. Even your 2-D simulation is valid to explain the triggering of kink-like flapping, the magnetopause disturbance is not the unique source. What I mean is that, the sources result in the pressure imbalance over tail current sheet could be multiple.

AC: We agree with the Referee. It is quite likely that occasionally there would be multiple hemispherically asymmetric signatures that could all result in a displacement of the current sheet. The result would probably be more irregular flapping signatures, which is not in disagreement with observations. We suggest to add on page 7, line 23: “Any hemispherically asymmetric magnetopause perturbation could cause tail flapping as shown here, but the shown perturbation initiated by subsolar magnetopause reconnection is a good example of a simulationally confirmed perturbation which indeed does cause this.”

Anonymous Referee #2

Received and published: 27 June 2018

AC = Liisa Juusola et al.,
Received and published: 27 June 2018

1. As you replied that your 2-D simulation cannot definitely differentiate which flapping type it is, it is only a potential candidate to explain the source to trigger the kink-like flapping, thus I think the title of your paper could be better changed as "A possible source mechanism for magnetotail flapping motion...".

AC: Please note that the title does not only refer to the kink-like flapping in the y direction but also flapping in the x-z plane. While the significance of our results as a source mechanism to the waves in y direction remains a point of discussion, we have shown that in the simulation the mechanism does indeed produce flapping in the x-z plane.

Nonetheless, we can change the title to "A possible source mechanism for magnetotail current sheet flapping".

2. Although you calculated the dBx/dt, Vz, the location of plasma sheet, and shown it in Figure 6, I did not see any comparisons between your simulation and the actual observation properties of flapping motion. I understand your simulation is 2-D, you are unable to compare the wavelength, propagation speed, etc., but you can compare the flapping period at least. From your Figure 3, Figure 6, your flapping period is about 2 hours, it is evidently much larger than the typical observed flapping period (10 mins). The simulation is a good tool to explore the physical mechanism, but I CANNOT accept it without any comparison with observations.

AC: Please note that the time in the figures in not given in HH:MM (hours and minutes) but MM:SS (minutes and seconds). This information is provided both in the caption of Figure 1 and on page 3, line 24 where this figure is first introduced. The captions of the following figures provide the information that they follow a format similar to that of Figure 1. However, as the notation was not clear, we are happy to include the explanation “, where MM indicates minutes and SS seconds” both on page 3, line 24 and in the caption of Figure 1.

We review many observational properties of current sheet flapping, including numerical values, in the Introduction. In section 3.1 we compare these numbers (including Bx and Vz) with those from our simulation, and find good agreement. The flapping period is compared with the observations of Sergeev et al. (1998) on page 3, lines 30-31.

3. As you agree with my comment that, the source could be multiple. Here, you only consider the case of solar wind that “Steady solar wind, characterized by Maxwellian distribution functions, proton density of 1 cm−3, temperature of 0.5 MK, velocity of −750 km/s along the x axis, and magnetic field of −5 nT along the z axis (purely southward IMF)”. Have you considered the other solar wind conditions, e.g. the northward IMF; the SW with a jump of dynamic pressure? I think you have to answer a question if your study is really important: Among the possible multiple sources, how much the case you studied contribute to the tail flapping motion?

AC: A particular set of solar wind conditions instead of a range of values was used because of the heavy computational load of running this type of a simulation. This same run has been analyzed in several previous studies as well (page 2, lines 23-25). The run was suitable for our study, because current sheet flapping occurred in it.

The question posed by the Referee is certainly interesting and a good topic for a future study. However, we consider it to be outside of the scope of the present paper.

Anonymous Referee #2
Received and published: 28 June 2018

I have no further comments.
I’m eager to see the revised paper as soon as possible.
To make the introduction full, two papers about the empirical flapping models could be cited for the better, and it could be beneficial for your future 3-D simulation.
1.Petrukovich, A.A., Baumjohann, W., Nakamura, R., Runov, A., 2008. Formation of current density profile in tilted current sheets. Ann. Geophys. 26, 3669–3676. 2.Rong, Z. J., C. Shen, A. A. Petrukovich, W. X. Wan, and Z. X. Liu (2010), The analytic properties of the ïňĆapping current sheets in the Earth magnetotail, Planet. Space Sci., 58(10), 1215–1229, doi:10.1016/j.pss.2010.04.016.

AC: -

A possible source mechanism for magnetotail current sheet flapping

Liisa Juusola[1,2], Yann Pfau-Kempf[1], Urs Ganse[1], Markus Battarbee[1], Thiago Brito[1], Maxime Grandin[1], Lucile Turc[1], and Minna Palmroth[1,2]

[1]University of Helsinki, Department of Physics, Helsinki, Finland
[2]Finnish Meteorological Institute, Helsinki, Finland

Correspondence: L. Juusola (liisa.juusola@fmi.fi)

Abstract. The origin of the flapping motions of the current sheet in the Earth's magnetotail is one of the most interesting questions of magnetospheric dynamics yet to be solved. We have used a polar plane simulation from the global hybrid-Vlasov model Vlasiator to study the characteristics and source of current sheet flapping in the center of the magnetotail. The characteristics of the simulated signatures agree with observations reported in the literature. The flapping is initiated by a hemispherically asymmetric magnetopause perturbation, created by subsolar magnetopause reconnection, that is capable of displacing the tail current sheet from its nominal position. The current sheet displacement propagates downtail at the same pace as the driving magnetopause perturbation. The initial current sheet displacement launches a standing magnetosonic wave within the tail resonance cavity. The travel time of the wave within the local cavity determines the period of the subsequent flapping signatures. Compression of the tail lobes due to added flux affects the cross-sectional width of the resonance cavity as well as the magnetosonic speed within the cavity. These in turn modify the wave travel time and flapping period. The compression of the resonance cavity may also provide additional energy to the standing wave, which may lead to strengthening of the flapping signature. ~~I~~It may be possible that the suggested mechanism could act as a source for kink-like waves that have been observed to be emitted from the center of the tail and to propagate toward the dawn and dusk flanks.

Keywords. Magnetosphere and space plasma physics (Magnetotail; Numerical simulation studies; Magnetospheric configuration and dynamics)

1 Introduction

The magnetotail current or neutral sheet is a relatively narrow region of lobe magnetic field reversal within a broader plasma sheet region between the tail lobes. A satellite on an orbit passing through this region often observes multiple current sheet crossings, indicating that the sheet moves ~~back and forth across~~up and down relative to the spacecraft several times. This flapping motion of the current sheet is observed as up to tens of nT variations in the magnetic field Geocentric Solar Magnetospheric (GSM) B_x component, often associated with a change of polarity of B_x (Speiser and Ness, 1967).

The temporal scale of the flapping variations ranges from tens of seconds to tens of minutes (Sergeev et al., 1998). The variations are interpreted as up and down motion of the current sheet with respect to the stationary satellite, such that $\partial B_x/\partial t$ anticorrelates with the GSM north component of the plasma bulk velocity (V_z). Sergeev et al. (1998) show example events with V_z varying from some tens of $\mathrm{km/s}$ to some hundreds of $\mathrm{km/s}$. The majority of the flapping events are observed during thin

current sheets within ± 10 min around substorm onset or intensification (Sergeev et al., 1998). Laitinen et al. (2007) presented an event during which current sheet oscillations were timed to occur both before tail reconnection and during it.

Two types of flapping motions have been distinguished: steady flapping and kink-like flapping (Rong et al., 2015). Steady flapping refers to oscillations in the z direction during which the current sheet normal remains more or less in the same direction. Such oscillations do not propagate as waves but remain stationary. The kink-like flapping, on the other hand, is able to propagate as waves. The sheet as a whole is tilted, rather than being locally expanded and contracted like in the sausage wave, which could also have explained the observed flapping signatures (Runov et al., 2003; Sergeev et al., 2003). The kink-like flapping may propagate along the y axis, in which case the current sheet normals for subsequent crossings vary the in $y-z$ plane, or along the x axis, so that the normals vary in $x-z$ plane (Rong et al., 2015; Sun et al., 2013). All three flapping types (steady flapping, kink-like along y, and kink-like along x) can yield similar time series of the B_x component.

Flapping has been observed as close to the Earth as 12 Earth radii ($\mathrm{R_E}$), i.e., close to the transition region or hinge point between tail-like and dipolar field lines (Sergeev et al., 1998). The waves are tail-aligned structures with the cross-tail wavelength ($\sim 5\ \mathrm{R_E}$) clearly smaller than the along-tail length ($> 10\ \mathrm{R_E}$) (Runov et al., 2009), and are observed to propagate toward the flanks from the center of the tail at velocities of some tens of $\mathrm{km/s}$ (Sergeev et al., 2004).

The origin of the flapping motion has not been established, although several tentative explanations, including solar wind variations (e.g., Speiser and Ness, 1967; Sergeev et al., 2008; Shen et al., 2008; Forsyth et al., 2009) and internal sources (e.g., Sergeev et al., 2004; Golovchanskaya and Maltsev, 2005; Zelenyi et al., 2009; Davey et al., 2012; Wei et al., 2015) have been suggested. Bursty Bulk Flows (BBFs), produced as outflows from tail reconnection, are among the suggested internal sources (Gabrielse et al., 2008; Erkaev et al., 2009). Statistical results have demonstrated that the occurrence rate of flapping motions is similar to that of BBFs, and peak in the central part of the magnetotail (Sergeev et al., 2006). Empirical models (Petrukovich et al., 2008; Rong et al., 2010) have been constructed to describe the characteristics of flapping current sheets.

In this study, we analyze a two-dimensional (2D) polar plane simulation produced using the global magnetospheric hybrid-Vlasov model Vlasiator[1]. The simulation is driven by steady solar wind, characterized by high solar wind speed and southward interplanetary magnetic field (IMF). About half an hour after the start of the simulation, tail reconnection begins. The same run has been used earlier to analyze subsolar magnetopause reconnection (Hoilijoki et al., 2017), onset of tail reconnection (Palmroth et al., 2017), and ion acceleration by flux transfer events in the magnetosheath (Jarvinen et al., 2018). Our aim is to examine the current sheet flapping signatures present in the simulation before and after the onset of tail reconnection, and to determine the driver of the flapping motions. Because the simulation is 2D, we concentrate on the characteristics and source of the waves in the center of the tail (i.e., waves in the $x-z$ plane). ~~We~~ We also discuss to possibility that in 3D, they could drive the kink-like waves that are emitted from the center of the tail and propagate dawnward and duskward (i.e., waves in the $y-z$ plane). The structure of the paper is as follows: the Vlasiator model is described in Section 2 and the results presented in Section 3. Section 4 contains discussion and Section 5 summarizes the conclusions.

[1] http://www.physics.helsinki.fi/vlasiator

2 Methods

We use the hybrid-Vlasov model Vlasiator (Palmroth et al., 2013; von Alfthan et al., 2014; Palmroth et al., 2015). In this version of the simulation, ions are modeled as 5D velocity distribution functions (2D in space, 3D in velocity) that are propagated in time according to Vlasov's equation. Ampère's law, Faraday's law, and generalized Ohm's law, including the Hall term, complete the set of equations. Electrons are neglected apart from their charge-neutralizing behavior.

The spatial resolution of the 2D polar plane simulation is $\Delta x = \Delta z = 300$ km or ~ 0.047 R_E (1 R_E = 6371 km) and the velocity space resolution $\Delta v_x = \Delta v_y = \Delta v_z = 30$ km/s. The velocity space in each spatial grid cell covers $v_x = v_y = v_z = \pm 4020$ km/s. The simulation box extends from $x = 300,000$ km or ~ 47 R_E on the dayside to $x = -600,000$ km or ~ -94 R_E on the nightside. In the north-south direction the box covers $z = \pm 360,000$ km or $\sim \pm 57$ R_E. The inner boundary of the simulation is at the distance of $30,000$ km or ~ 5 R_E from the origin. The geomagnetic field is modeled as a 2D line dipole that is centered at the origin, aligned with the z axis, and scaled toresult in a realistic magnetopause standoff distance (Daldorff et al., 2014). Thus, the coordinate system is comparable to GSM.

Steady solar wind, characterized by Maxwellian distribution functions, proton density of 1 cm^{-3}, temperature of 0.5 MK, velocity of -750 km/s along the x axis, and magnetic field of -5 nT along the z axis (purely southward IMF), is fed into the simulation box from its sunward wall ($+x$). Copy-conditions are applied to the other outer walls ($-x$, $\pm z$), and periodic boundary conditions to the out-of-plane ($\pm y$) directions. The inner boundary enforces a static Maxwellian velocity distribution and perfect conductor field boundary conditions. The simulation output (moments and fields) is saved every simulated 0.5 s.

3 Results

In this section, we start (section 3.1) by examining the characteristics of the current sheet flapping signatures in the simulation and by comparing them with the observations cited in the Introduction. After that (section 3.2), we suggest a mechanism that could explain how the flapping motion is initated and maintained.

Fig. 1 introduces the $x-z$ plane simulation by showing a snap-shot at 19 min and 40 s after the start of the run. The background color displays ratio of the ion thermal pressure perpendicular to the magnetic field and the magnetic pressure ($\beta_\perp = P_{thermal,\perp}/P_{magnetic}$). Closed magnetic field lines are drawn as green curves, semi-open field lines (with one footpoint at the inner boundary) as black curves, and open field lines as gray curves. Field lines that are closed but not attached to the geomagnetic field are drawn in magenta. The tail lobes are estimated to lie between the blue curves. These curves indicate the innermost boundaries where $\beta_\perp > 1$ in the region $|z| > 5$ R_E and $x < 0$. This proxy is based on the assumption that while the magnetosheath is dominated by the plasma pressure, the tail lobes are magnetically dominated. At the time shown, a hemispherically asymmetric magnetopause perturbation, created around the time when subsolar reconnection first started to add new semi-open flux tubes to the lobes, has reached the distance $x \approx -40$ R_E (inside the red box). The significance of this perturbation will be discussed further in section 3.2.

3.1 Characteristics of current sheet flapping signatures

Figure 2 shows the earthward component of the magnetic field (B_x, color) at the nominal location of the magnetotail current sheet ($y = z = 0$) as a function of x and time (MM:SS, where MM indicates minutes and SS seconds). The tilted black lines indicate motion at the solar wind velocity $V_x = -750$ km/s. The vertical black lines at 19:40 and 27:00 mark the time of Fig. 1 and the onset time of tail reconnection at $x \approx -14$ R_E (Palmroth et al., 2017), respectively. The most striking feature in the plot is the alternating positive and negative enhancements of B_x of the order of 10 nT in amplitude. The signatures first appear in the transition region and subsequently propagate tailward at a velocity which is generally close to the solar wind velocity as indicated by the tilted black lines. The B_x enhancements can appear fairly regular for a while (e.g., around $x = -40$ R_E between 24:00 and 30:00) or quite irregular (e.g., tailward of $x = -50$ R_E). The durations of the enhancements at a given location vary from a few minutes to less than a minute, in agreement with Sergeev et al. (1998). The along-tail lengths of the signatures vary, but can be > 10 R_E, in agreement with Runov et al. (2009). The enhancements occur for $\sim$13 min before the onset of tail reconnection as indicated by the vertical black line, and can be observed at least for $\sim$4 min after, in agreement with Sergeev et al. (1998) and Laitinen et al. (2007), before the signatures are disrupted by the spreading effects of tail reconnection. After this, B_x enhancements can still be observed between -30 and -10 R_E until the end of the simulation, i.e., 9 min after the onset of reconnection.

The B_x signatures resemble those associated with current sheet flapping, discussed in the Introduction. In order to check whether this might indeed be the case, Fig. 3 shows the time derivative of B_x ($\partial B_x/\partial t$) and Fig. 4 the z component of the ion bulk velocity (V_z). The cyan curves in Fig. 4 indicate isocontours of pressure in the z direction ($P_{magnetic,z} + P_{thermal,z}$) with a thicker curve indicating higher pressure (levels 0.05 nPa, 0.1 nPa, and 0.2 nPa). The curves have only been plotted in the tail-like region undisturbed by significant effects from tail reconnection. The magenta dots in Fig. 4 mark flapping half periods at $x = -30$ R_E, $x = -40$ R_E, and $x = -65$ R_E, identified based on sign changes of V_z. Comparison of Fig. 3 and Fig. 4 shows that V_z and $\partial B_x/\partial t$ are anticorrelated (this can also be seen in Fig. 7 below), implying that the variations in B_x are caused by up and down motion of the current sheet with respect to the $z = 0$ plane (Sergeev et al., 1998). The amplitude of V_z is also in agreement with the observations of Sergeev et al. (1998).

Fig. 4 illustrates that while the first significant signature of downward ion bulk flow (blue) propagates all the way through the tail at a speed very close to the solar wind speed, the tailward propagation of the subsequent signatures is disrupted at some x distances (e.g., around $x \approx -55$ R_E at 28:00). These x distances are not constant but they appear to propagate tailward as well, although more slowly than the flapping signatures. Furthermore, the characteristic period of the flapping appears to change at these locations such that signatures closer to the Earth have a smaller characteristic period than those farther down the tail. The characteristic period within a given region also seems to decrease with increasing time. The cyan curves indicating isocontours of pressure reveal that the changes appear to be related to pressure, such that in regions of higher pressure the period of the signatures is smaller. The pressure increase with increasing time is caused by subsolar reconnection adding semi-open magnetic flux to the lobes before tail reconnection starts to close it efficiently enough (Palmroth et al., 2017).

Fig. 5 and Fig. 6 show the location and thickness of the plasma sheet in the z direction, respectively. The plasma sheet extent in z as a function of x and time was identified as the region between $z = \pm 10$ R_E where the ion thermal pressure perpendicular to the magnetic field is larger than magnetic pressure ($\beta_\perp = P_{thermal,\perp}/P_{magnetic} > 1$) (e.g., Wang et al., 2006). The z coordinate was obtained as the mean of the largest and smallest plasma sheet z value, and the thickness as their difference. Gray areas in the plots indicate regions where the condition $\beta_\perp > 1$ was not met anywhere between $z = \pm 10$ R_E. Comparison of Fig. 5 with Fig. 2 shows good correlation between the plasma sheet motion and B_x enhancements, confirming that the enhancements are indeed produced by up and down motion of the plasma sheet. The extent of the motion in z direction is not very large, less than 1 R_E, in agreement with Speiser and Ness (1967), but because the plasma sheet is thin (Fig. 6), this produces significant changes in B_x.

Finally, before moving on to discuss the drivers of plasma sheet flapping, Fig. 7 shows a time series observed by a virtual satellite located at $x = -40$ R_E and $y = z = 0$ in the simulation. From top to bottom, the parameters shown are: B_x, $\partial B_x/\partial t$, V_z, and plasma sheet z location. The vertical magenta lines identify flapping half periods based on sign changes of V_z, and they correspond to the magenta dots at $x = -40$ R_E in Fig. 4. This plot further clarifies the mutual temporal behavior of the parameters and may be more straightforward to compare with real satellite observations (e.g., Sergeev et al., 1998) than the color map plots.

3.2 A driving mechanism for current sheet flapping

~~Fig. 1 shows $\beta_\perp$ and magnetic field lines in the $x - z$ plane at 19:40. Closed field lines are drawn in green, semi-open field lines (with one footpoint at the inner boundary) in black, and open field lines in gray. Field lines that are closed but not attached to the geomagnetic field are drawn in magenta. The tail lobes are estimated to lie between the blue curves. These curves indicate the innermost boundaries where $\beta_\perp > 1$ in the region $|z| > 5$ R_E and $x < 0$. This proxy is based on the assumption that while the magnetosheath is dominated by the plasma pressure, the tail lobes are magnetically dominated.~~ At the time shown in Fig. 1, a hemispherically asymmetric magnetopause perturbation, created around the time when subsolar reconnection first started to add new semi-open flux tubes to the lobes, has reached the distance $x \approx -40$ R_E (inside the red box). The asymmetric perturbation consists of a simultaneous compression of the northern tail lobe and expansion of the southern tail lobe. The current sheet between the lobes has been shifted slightly southward from its nominal position at $z = 0$. This shift corresponds to the first strong flapping signature (red, starting around $x \approx -15$ R_E at ~16:00) in Fig. 2.

Fig. 8 shows V_z as a function of z and time at $y = 0$ and $x = -40$ R_E. The vertical black lines are the same as in Fig. 2. The white and magenta (only plotted until 31:00) curves indicate the innermost boundaries where $\beta_\perp > 1$ and $\beta_\perp > 0.1$ in the region $|z| > 5$ R_E, respectively. The tail lobes are estimated to lie between the white curves (corresponding to the blue curves in Fig. 1).

Fig. 8 shows that typically V_z is directed toward the plasma sheet in both lobes. Close (roughly within $z = \pm 5$ R_E) to the plasma sheet where the flapping produces alternating positive and negative values of V_z in both hemispheres (~24:00–30:00). Close to the magnetopause where localized compressions (e.g., around $z = 23$ R_E at 14:00–16:00) and expansions (e.g., around $z = 23$ R_E at 16:00–18:00) cause plasma flow toward and away from the plasma sheet, respectively. Furthermore, after

24:00 the magnetopause starts to expand outward due to the accumulation of magnetic flux recently opened by the subsolar reconnection. In these regions, V_z still reflects the motion of the solar wind and is thus directed away from the plasma sheet. The magenta curves in the plot roughly estimate the boundaries between the pre-existing lobe field lines and the newly added lobe field lines.

Fig. 8 reveals that the passage of the hemispherically asymmetric magnetopause perturbation at the time when the flapping starts around $x = -40$ $\mathrm{R_E}$ is a unique incident. The simultaneous compression of the northern lobe and expansion of the southern lobe causes a downward plasma flow across the entire tail between ∼18:00 and 20:00, which leads to the current sheet shifting downward into the southern hemisphere. Only this first flapping signature appears to have a clear magnetopause driver. In order to find out what causes the flapping to continue after the initial driver has passed, Fig. 9 shows the time derivative of B_x in the same format as Fig. 8. At the start of the flapping between 18:00 and 20:00, there is a blue signature in both lobes close to the plasma sheet. This is related to positive B_x in the northern lobe weakening and negative B_x in the southern lobe strengthening. Very close to the plasma sheet the signature is positive as the previously close to zero B_x of the current sheet is replaced by positive B_x as the sheet moves downward. For several minutes (∼20:00–24:00) after this clear initial signature the time derivative of B_x in the lobes consists of small-scale structures, until more coherent, larger-scale signatures associated with strong flapping are established after ∼24:00. The small-scale structure of $\partial B_x/\partial t$ in the lobes between the initial magnetopause driver and subsequent establishment of the flapping strongly suggests wave activity between the plasma sheet and the magenta curves.

The magnetotail acts both like a waveguide and a resonance cavity (McPherron, 2005). Alfvén waves that tend to propagate down the tail wave guide along the background lobe magnetic field lines are eventually lost. Magnetosonic waves that propagate perpendicular to the background magnetic field can form standing waves in the tail resonance cavity at a roughly constant distance from the Earth. A tailward propagating displacement of the boundary of the cavity produces a disturbance inside the magnetosphere that stands in the ~~cross-tail~~$x - z$ direction while propagating down the tail. Fig. 10 shows the magnetosonic speed (V_{ms}) across the tail at the distance $x = -40$ $\mathrm{R_E}$. There is a distinct change in the magnetosonic speed near the location of the magenta curves. This would explain why the waves if Fig. 9 appear to reflect there. We estimate that the magnetosonic wave resonance cavity lies between these curves.

Standing waves are only possible at discrete frequencies. The simplest approximation to the fundamental period can be obtained by integrating the magnetosonic travel time $dt = dz/V_{ms}$ across the cavity (or back and forth across one hemisphere of the cavity). Fig. 11 shows the travel time across half of the magnetotail resonance cavity ($T/2$) at distances $x = -30$ $\mathrm{R_E}$ (black), $x = -40$ $\mathrm{R_E}$ (red), and $x = -65$ $\mathrm{R_E}$ (blue) as a function of time (solid curves). For example, $T/2$ at $x = -40$ $\mathrm{R_E}$ has been estimated by integrating $dt = dz/V_{ms}$ over the distance between the magenta curves marked in Fig. 10 and dividing by 2. The dots in Fig. 11 indicate tail flapping half periods with color indicating the corresponding x-coordinate. The flapping half periods have been obtained as the time differences between consecutive magenta dots indicated in Fig. 4, and they have been associated with a time stamp corresponding to the average of the two times. The dashed vertical lines mark the start and end time of the first flapping signature at the three distances.

The travel time at a given distance decreases with increasing time as the increase in pressure due to the addition of flux tubes opened by subsolar reconnection compresses the lobes, decreasing the cross section of the cavity and increasing the magnetosonic speed within. The bumps in the travel time during the first flapping signature at all three x distances are associated with the magnetopause perturbation that initiated the flapping. Apart from the first flapping signature at a given distance, there appears to be a good correspondence between the approximated local magnetosonic travel time across half of the resonance cavity and the observed flapping half period. Both Fig. 11 and Fig. 4 show that the period of the flapping signatures increases with increasing distance away from the Earth. At a given location, the period decreases with increasing time. These changes follow the structure and development of pressure indicated in Fig. 4 by the cyan curves. Higher pressure indicates smaller cross-section of the cavity and higher magnetosonic speed due to the higher magnetic field strength, which is in agreement with the suggestion that the local flapping period is determined by the bounce time of the magnetosonic waves within the cavity.

4 Discussion

We have examined current sheet flapping in Vlasiator and suggested a source mechanism that is capable of initiating and maintaining flapping in the central meridian of the magnetotail before and during tail reconnection when the plasma sheet is thin. According to our suggested mechanism, the flapping is initiated by a hemispherically asymmetric perturbation of the magnetopause that is capable of displacing the current sheet from its nominal position. The perturbation travels tailward along the magnetopause (close to the solar wind speed in this case), producing a current sheet displacement that propagates tailward at the same speed. As the first flapping signature is directly driven by the magnetopause perturbation, no correspondence between the duration of flapping signature and the local magnetosonic wave travel time in Fig. 11 is expected. The initial current sheet displacement launches a standing magnetosonic wave within the local resonance cavity. The travel time of the wave within the cavity determines the period of the subsequent flapping signatures, as shown in Fig. 11. Changes in the cross-sectional width of the cavity as well as the magnetosonic speed within the cavity affect the wave travel time and thus the local flapping period. The flapping signatures that can be produced by our suggested mechanism are compliant with the characteristics of plasma sheet flapping in the center of the tail cited in the Introduction.

We do not observe a damping of the current sheet flapping. On the contrary, after the initial displacement, the signature can even strengthen (e.g., at $x = -40$ $\mathrm{R_E}$ in 24:00–28:00 in Fig. 2). The reason for this could be the continued compression of the cavity that could provide additional energy to the standing wave.

In our polar plane simulation driven by steady solar wind, the initiating magnetopause perturbation is created by subsolar reconnection. In 3D, such a perturbation could have a finite extent in the y direction, and propagate tailward along the noon-midnight sector magnetopause. Thus, the created plasma sheet flapping in the midnight sector plasma sheet could act as a source for the dawnward and duskward propagating flapping signatures that have been observed by satellites (e.g., Sergeev et al., 2004). A solar wind perturbation, such as a tilted interplanetary shock, might also be able to produce the initial plasma sheet displacement, but probably not in such a localized manner (in y), as solar wind structures tend to be of much larger scale

sizes. Any hemispherically asymmetric magnetopause perturbation could cause tail flapping as presented here, but the shown perturbation initiated by subsolar magnetopause reconnection is a good example of a perturbation confirmed by simulation which indeed does cause this. However, the perturbation initiating the flapping need not necessarily be at the magnetopause. Any disturbance capable of displacing the current sheet, a BBF for example, should be able to initiate the flapping.

For the purposes of further validation against satellite observations, our model predicts that, e.g., the flapping period at a given observation location should decrease with increasing pressure in the lobes.

5 Conclusions

We have used a polar plane simulation from the global hybrid-Vlasov model Vlasiator, driven by steady southward IMF and fast solar wind, to study the characteristics and source of current sheet flapping signatures in the magnetotail. Because the simulation is 2D, we concentrated on the flapping in the center of the tail. Our main results are as follows:

1. The characteristics of the simulated flapping signatures agree with observations reported in the literature.
2. In the simulation, the flapping is initiated by a hemispherically asymmetric magnetopause perturbation, created by subsolar reconnection, that is capable of displacing the tail current sheet from its nominal position. The current sheet displacement propagates downtail together with the driving magnetopause perturbation.
3. As the intial current sheet displacement passes, it launches a standing magnetosonic wave within the local tail resonance cavity. The travel time of the wave within the cavity determines the period of the subsequent flapping signatures.
4. Increasing pressure in the tail lobes due to an increasing amount of open magnetic flux added by subsolar reconnection can affect the cross-sectional width of the resonance cavity as well as the magnetosonic speed within the cavity. These in turn affect the wave travel time and flapping period. The compression of the resonance cavity may also provide additional energy to the standing wave, which may lead to strengthening of the flapping signature.
5. ~~The suggested mechanism could act as a source for kink-like waves that are emitted from the center of the tail and propagate toward the dawn and dusk flanks. In 3D, the initial driving magnetopause perturbation created by subsolar reconnection could have a finite dawn-dusk extent, possibly corresponding to the width of the subsolar reconnection line.~~

The suggested mechanism could act as a source for kink-like waves that are emitted from the center of the tail and propagate toward the dawn and dusk flanks. However, further research using a 3D simulation will be needed to examine this suggestion.

Code availability. Vlasiator is an open source code released under the GPLv2 license. The code is available at http://github.com/fmihpc/vlasiator.

Author contributions. LJ carried out most of the analysis and prepared the manuscript. YP-K participated in running the simulation and development of the analysis methods. UG participated in development of the analysis methods. All co-authors read the manuscript and commented on it.

Competing interests. The authors declare that they have no conflict of interest.

Acknowledgements. We acknowledge The European Research Council for Starting grant 200141-QuESpace, with which Vlasiator (http://www.physics.helsinki.fi/vlasiator) was developed, and Consolidator grant 682068-PRESTISSIMO awarded for further development of Vlasiator and its use in scientific investigations. We gratefully acknowledge Academy of Finland grants number 267144 and 309937. The work leading to these results has been partially carried out in the Finnish Centre of Excellence in Research of Sustainable Space (Academy of Finland grant number 312351). PRACE (http://www.prace-ri.eu) is acknowledged for granting us Tier-0 computing time in HLRS Stuttgart, where Vlasiator was run in the HazelHen machine with project number 2014112573. The work of LT is supported by a Marie Sklodowska-Curie Individual Fellowship (#704681).

References

Daldorff, L. K. S., Tóth, G., Gombosi, T. I., Lapenta, G., Amaya, J., Markidis, S., and Brackbill, J. U.: Two-way coupling of a global Hall magnetohydrodynamics model with a local implicit particle-in-cell model, Journal of Computational Physics, 268, 236–254, https://doi.org/https://doi.org/10.1016/j.jcp.2014.03.009, 2014.

Davey, E. A., Lester, M., Milan, S. E., and Fear, R. C.: Storm and substorm effects on magnetotail current sheet motion, J. Geophys. Res., 117, A02202, https://doi.org/10.1029/2011JA017112, 2012.

Erkaev, N. V., Semenov, V. S., Kubyshkin, I. V., Kubyshkina, M. V., and Biernat, H. K.: MHD model of the flapping motions in the magnetotail current sheet, J. Geophys. Res., 114, A03206, https://doi.org/10.1029/2008JA013728, 2009.

Forsyth, C., Lester, M., Fear, R. C., Lucek, E., Dandouras, I., Fazakerley, A. N., Singer, H., and Yeoman, T. K.: Solar wind and substorm excitation of the wavy current sheet, Ann. Geophys., 27, 2457–2474, https://doi.org/10.5194/angeo-27-2457-2009, https://www.ann-geophys.net/27/2457/2009/, 2009.

Gabrielse, C., Angelopoulos, V., Runov, A., Kepko, L., Glassmeier, K. H., Auster, H. U., McFadden, J., Carlson, C. W., and Larson, D.: Propagation characteristics of plasma sheet oscillations during a small storm, Geophys. Res. Lett., 35, L17S13, https://doi.org/10.1029/2008GL033664, 2008.

Golovchanskaya, I. V. and Maltsev, Y. P.: On the identification of plasma sheet flapping waves observed by Cluster, Geophys. Res. Lett., 32, L02102, https://doi.org/10.1029/2004GL021552, 2005.

Hoilijoki, S., Ganse, U., Pfau-Kempf, Y., Cassak, P. A., Walsh, B. M., Hietala, H., von Alfthan, S., and Palmroth, M.: Reconnection rates and X line motion at the magnetopause: Global 2D-3V hybrid-Vlasov simulation results, J. Geophys. Res. Space Physics, 122, https://doi.org/10.1002/2016JA023709, 2017.

Jarvinen, R., Vainio, R., Palmroth, M., Juusola, L., Hoilijoki, S., Pfau-Kempf, Y., Ganse, U., Turc, L., and von Alfthan, S.: Ion acceleration by flux transfer events in the terrestrial magnetosheath, Geophys. Res. Lett., 45, https://doi.org/https://doi.org/10.1002/2017GL076192, 2018.

Laitinen, T. V., Nakamura, R., Runov, A., Rème, H., and Lucek, E. A.: Global and local disturbances in the magnetotail during reconnection, Ann. Geophys., 25, 1025–1035, https://doi.org/https://doi.org/10.5194/angeo-25-1025-2007, 2007.

McPherron, R. L.: Magnetic Pulsations: Their Sources and Relationto Solar Wind and Geomagnetic Activity, Surveys in Geophysics, 26, 545–592, https://doi.org/10.1007/s10712-005-1758-7, 2005.

Palmroth, M., Honkonen, I., Sandroos, A., Kempf, Y., von Alfthan, S., and Pokhotelov, D.: Preliminary testing of global hybrid-Vlasov simulation: Magnetosheath and cusps under northward interplanetary magnetic field, Journal of Atmospheric and Solar-Terrestrial Physics, 99, 41–46, https://doi.org/http://dx.doi.org/10.1016/j.jastp.2012.09.013, 2013.

Palmroth, M., Archer, M., Vainio, R., Hietala, H., Pfau-Kempf, Y., Hoilijoki, S., Hannuksela, O., Ganse, U., Sandroos, A., von Alfthan, S., and Eastwood, J. P.: ULF foreshock under radial IMF: THEMIS observations and global kinetic simulation Vlasiator results compared, J. Geophys. Res. Space Physics, 120, 8782–8798, https://doi.org/10.1002/2015JA021526, 2015.

Palmroth, M., Hoilijoki, S., Juusola, L., Pulkkinen, T. I., Hietala, H., Pfau-Kempf, Y., Ganse, U., von Alfthan, S., Vainio, R., and hesse, M.: Tail reconnection in the global magnetospheric context: Vlasiator first results, Ann. Geophys., 35, 1269–1274, https://doi.org/https://doi.org/10.5194/angeo-35-1269-2017, 2017.

Petrukovich, A. A., Baumjohann, W., Nakamura, R., and Runov, A.: Formation of current density profile in tilted current sheets, Ann. Geophys., 26, 3669–3676, https://doi.org/10.5194/angeo-26-3669-2008, https://www.ann-geophys.net/26/3669/2008/, 2008.

Rong, Z. J., Shen, C., Petrukovich, A. A., Wan, W. X., and Liu, Z. X.: The analytic properties of the flapping current sheets in the earth magnetotail, Planetary and Space Science, 58, 1215–1229, https://doi.org/https://doi.org/10.1016/j.pss.2010.04.016, 2010.

Rong, Z. J., Barabash, S., Stenberg, G., Futaana, Y., Zhang, T. L., Wan, W. X., Wei, Y., and Wang, X.-D.: Technique for diagnosing the flapping motion of magnetotail current sheets based on single-point magnetic field analysis, J. Geophys. Res. Space Physics, 120, 3462–3474, https://doi.org/10.1002/2014JA020973, 2015.

Runov, A., Nakamura, R., Baumjohann, W., Zhang, T. L., Volwerk, M., Eichelberger, H.-U., and Balogh, A.: Cluster observation of a bifurcated current sheet, Geophys. Res. Lett., 30, 1036, https://doi.org/10.1029/2002GL016136, 2003.

Runov, A., Angelopoulos, V., Sergeev, V. A., Glassmeier, K.-H., Auster, U., McFadden, J., Larson, D., and Mann, I.: Global properties of magnetotail current sheet flapping: THEMIS perspectives, Ann. Geophys., 27, 319–328, https://doi.org/10.5194/angeo-27-319-2009, 2009.

Sergeev, V., Angelopoulos, V., Carlson, C., and Sutcliffe, P.: Current sheet measurements within a flapping plasma sheet, J. Geophys. Res., 103(A5), 9177–9187, https://doi.org/10.1029/97JA02093, 1998.

Sergeev, V., Runov, A., Baumjohann, W., Nakamura, R., Zhang, T. L., Volwerk, M., Balogh, A., Rème, H., Sauvaud, J. A., André, M., and Klecker, B.: Current sheet flapping motion and structure observed by Cluster, Geophys. Res. Lett., 30, 1327, https://doi.org/10.1029/2002GL016500, 2003.

Sergeev, V., Runov, A., Baumjohann, W., Nakamura, R., Zhang, T. L., Balogh, A., Louarn, P., Sauvaud, J.-A., and Réme, H.: Orientation and propagation of current sheet oscillations, Geophys. Res. Lett., 31, L05807, https://doi.org/10.1029/2003GL019346, 2004.

Sergeev, V. A., Sormakov, D. A., Apatenkov, S. V., Baumjohann, W., Nakamura, R., Runov, A. V., Mukai, T., and Nagai, T.: Survey of large-amplitude flapping motions in the midtail current sheet, Ann. Geophys., 24, 2015–2024, https://doi.org/https://doi.org/10.5194/angeo-24-2015-2006, 2006.

Sergeev, V. A., Tsyganenko, N. A., and Angelopoulos, V.: Dynamical response of the magnetotail to changes of the solar wind direction: an MHD modeling perspective, Ann. Geophys., 26, 2395–2402, https://doi.org/https://doi.org/10.5194/angeo-26-2395-2008, 2008.

Shen, C., Rong, Z. J., Li, X., Dunlop, M., Liu, Z. X., Malova, H. V., Lucek, E., and Carr, C.: Magnetic configurations of the tilted current sheets in magnetotail, Ann. Geophys., 26, 3525–3543, https://doi.org/10.5194/angeo-26-3525-2008, https://www.ann-geophys.net/26/3525/2008/, 2008.

Speiser, T. W. and Ness, N. F.: The neutral sheet in the geomagnetic tail: Its motion, equivalent currents, and field line connection through it, J. Geophys. Res., 72(1), 131–141, https://doi.org/10.1029/JZ072i001p00131, 1967.

Sun, W.-J., Fu, S., Shi, Q., Zong, Q.-G., Yao, Z., Xiao, T., and Parks, G.: THEMIS observation of a magnetotail current sheet flapping wave, Chinese Science Bulletin, 59, 154–161, 2013.

von Alfthan, S., Pokhotelov, D., Kempf, Y., Hoilijoki, S., Honkonen, I., Sandroos, A., and Palmroth, M.: Vlasiator: First global hybrid-Vlasov simulations of Earth's foreshock and magnetosheath, Journal of Atmospheric and Solar-Terrestrial Physics, 120, 24–35, https://doi.org/http://dx.doi.org/10.1016/j.jastp.2014.08.012, 2014.

Wang, C., Lyons, L. R., Weygand, J. M., Nagai, T., and McEntire, R. W.: Equatorial distributions of the plasma sheet ions, their electric and magnetic drifts, and magnetic fields under different interplanetary magnetic field Bz conditions, J. Geophys. Res., 111, A04215, https://doi.org/10.1029/2005JA011545, 2006.

Wei, X. H., Cai, C. L., Cao, J. B., Rème, H., Dandouras, I., and Parks, G. K.: Flapping motions of the magnetotail current sheet excited by nonadiabatic ions, Geophys. Res. Lett., pp. 4731–4735, https://doi.org/10.1002/2015GL064459, 2015.

Zelenyi, L. M., Artemyev, A. V., Petrukovich, A. A., Nakamura, R., Malova, H. V., and Popov, V. Y.: Low frequency eigenmodes of thin anisotropic current sheets and Cluster observations, Ann. Geophys., 27, 861–868, https://doi.org/https://doi.org/10.5194/angeo-27-861-2009, 2009.

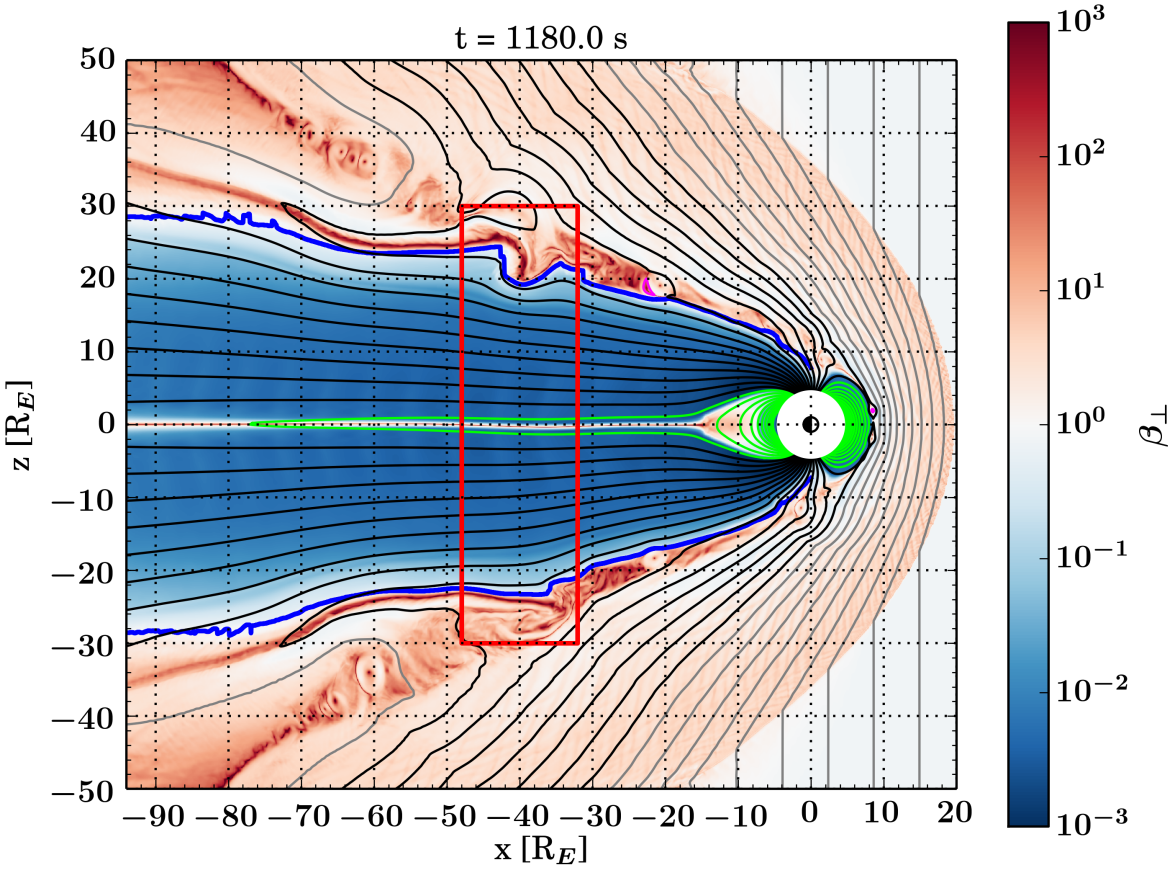

Figure 1. Ratio of ion thermal pressure prependicular to the magnetic field and magnetic pressure $\beta_\perp = P_{thermal,\perp}/P_{magnetic}$ and magnetic field lines in the $x-z$ plane at 19:40 (1180.0 s). Closed field lines are drawn in green, semi-open field lines in black, and open field lines in gray. Field lines that are closed but not attached to the geomagnetic field are drawn in magenta. The tail lobes are estimated to lie between the blue curves. The curves indicate the innermost boundaries where $\beta_\perp > 1$ in the region $|z| > 5$ $\mathrm{R_E}$ and $x < 0$. Inside the red box, a hemispherically asymmetric magnetopause perturbation compresses the northern tail lobe and expands the southern tail lobe, causing the current sheet between the tail lobes around $x = -40$ $\mathrm{R_E}$ to shift slightly southward from its nominal position at $z = 0$.

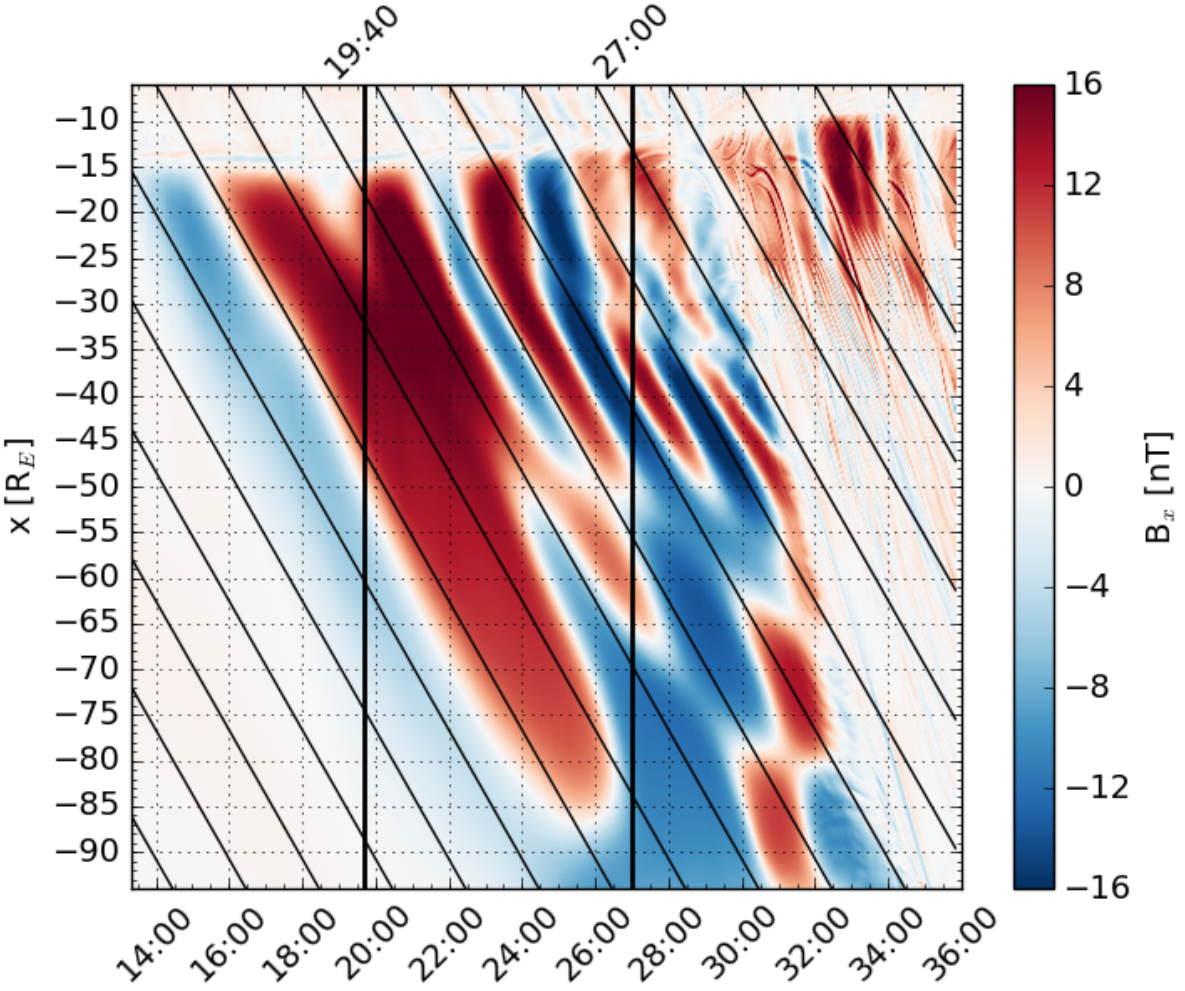

Figure 2. Earthward component of the magnetic field (B_x, color) at the nominal position of the tail current sheet ($y = z = 0$) as a function of x and time (MM:SS, where MM indicates minutes and SS seconds). The tilted black lines indicate motion at the solar wind velocity $V_x = -750$ km/s. The vertical black lines at 19:40 and 27:00 mark the time of Fig. 1 and the onset time of tail reconnection at $x \approx -14$ R_E, respectively.

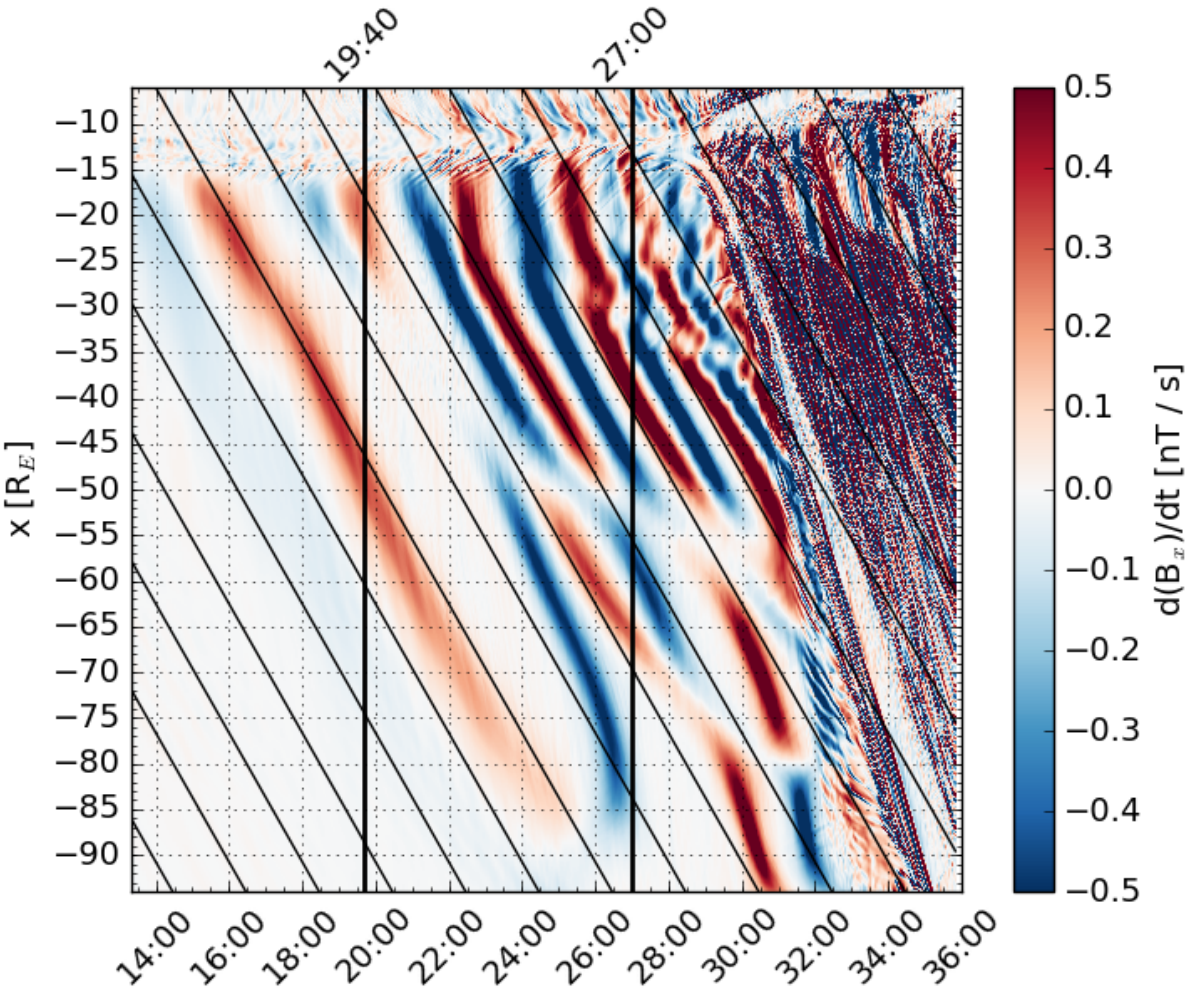

Figure 3. The same as Fig. 2 except that the color shows the time derivative of B_x. The color scale has been saturated to better show the relevant structures.

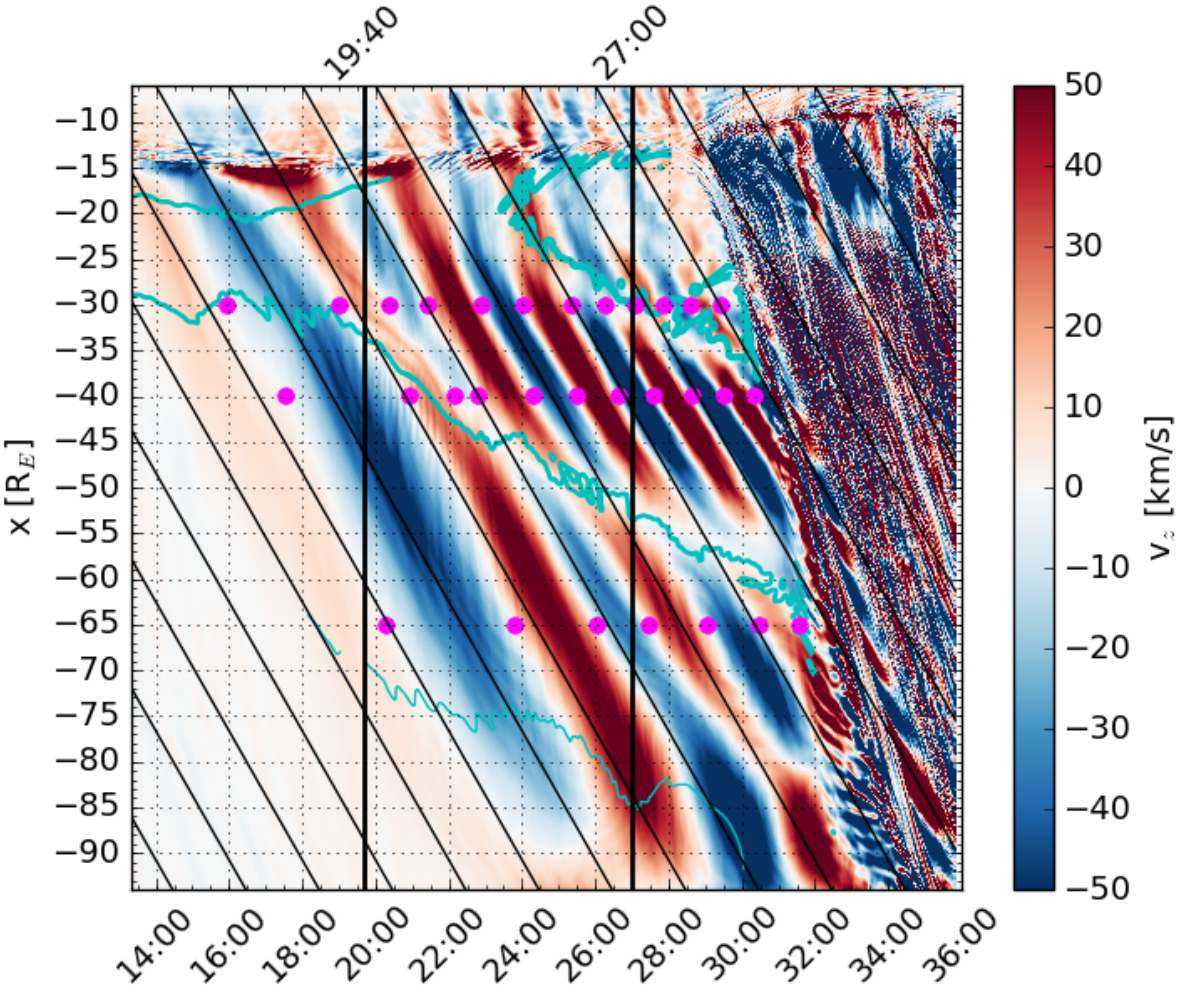

Figure 4. The same as Fig. 2 except that the color shows the north component of the ion bulk velocity (V_z). The cyan curves indicate isocontours of pressure in the z direction ($P_{magnetic,z} + P_{thermal,z}$) with a thicker curve indicating higher pressure: 0.05 nPa, 0.1 nPa, and 0.2 nPa. The magenta dots mark identified flapping half periods at $x = -30$ R$_E$, $x = -40$ R$_E$, and $x = -65$ R$_E$.

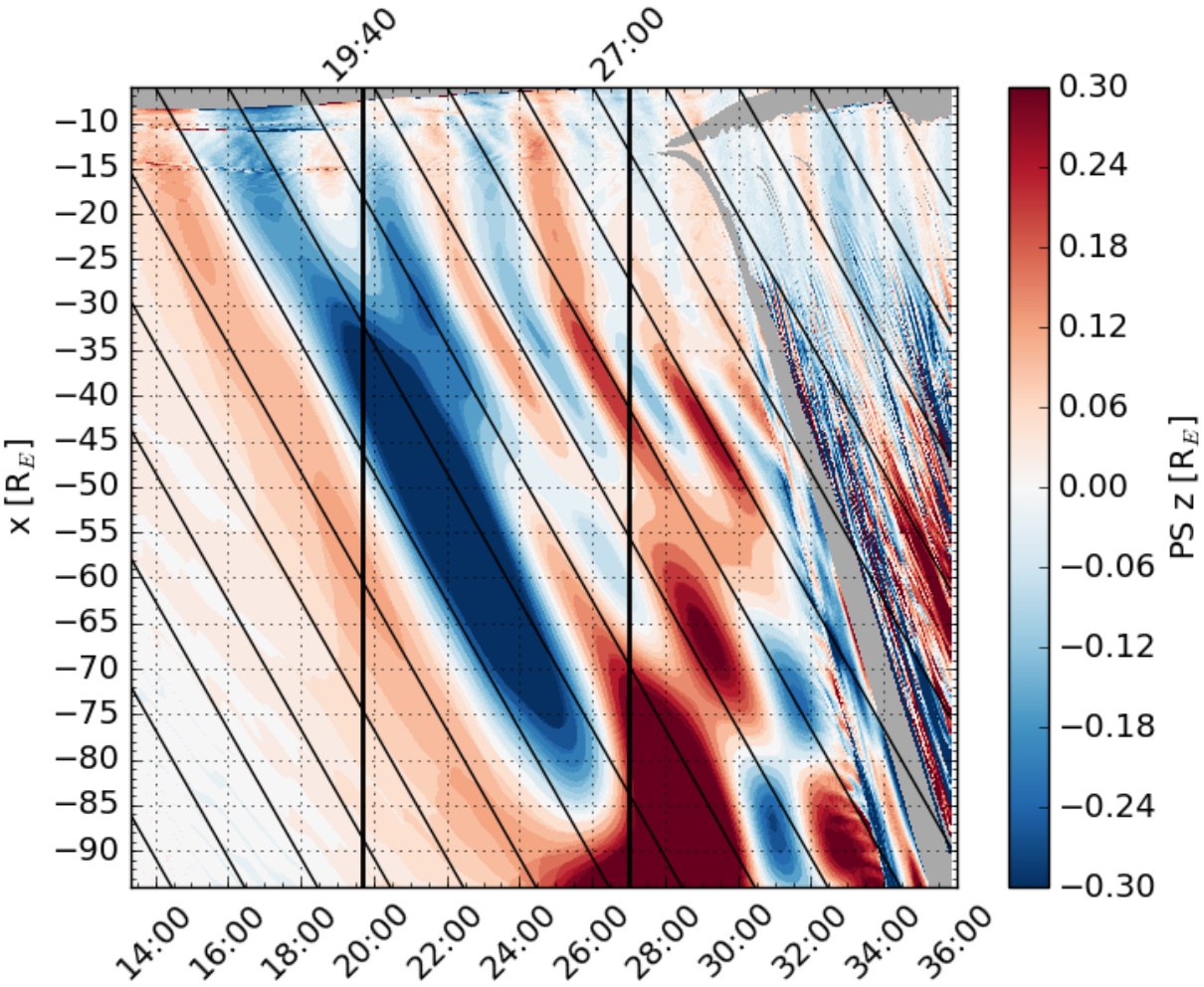

Figure 5. The same as Fig. 2 except that the color shows the location of the plasma sheet center in the z direction. Gray areas indicate regions where the location could not be determined.

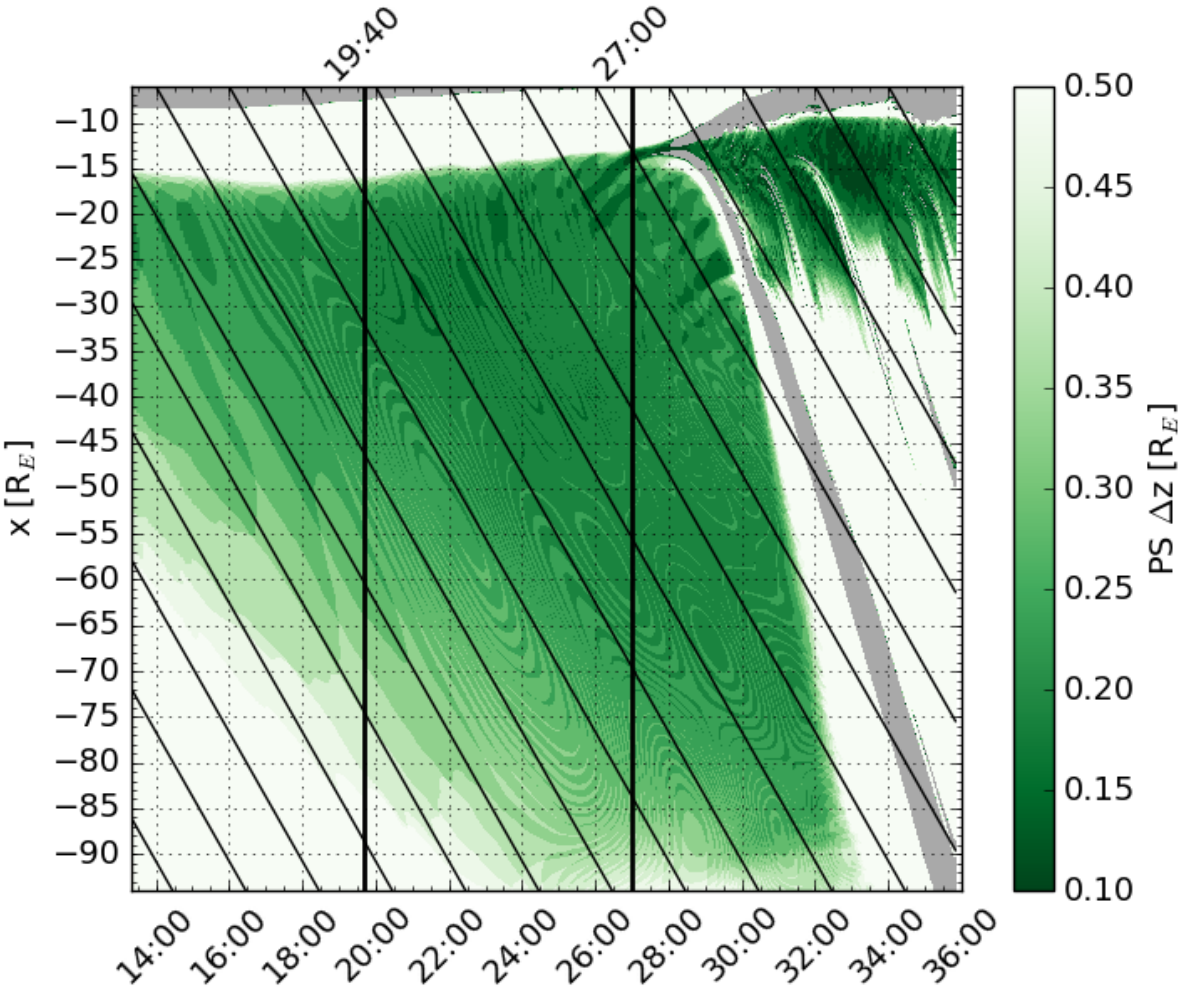

Figure 6. The same as Fig. 5 except that the color shows the plasma sheet thickness.

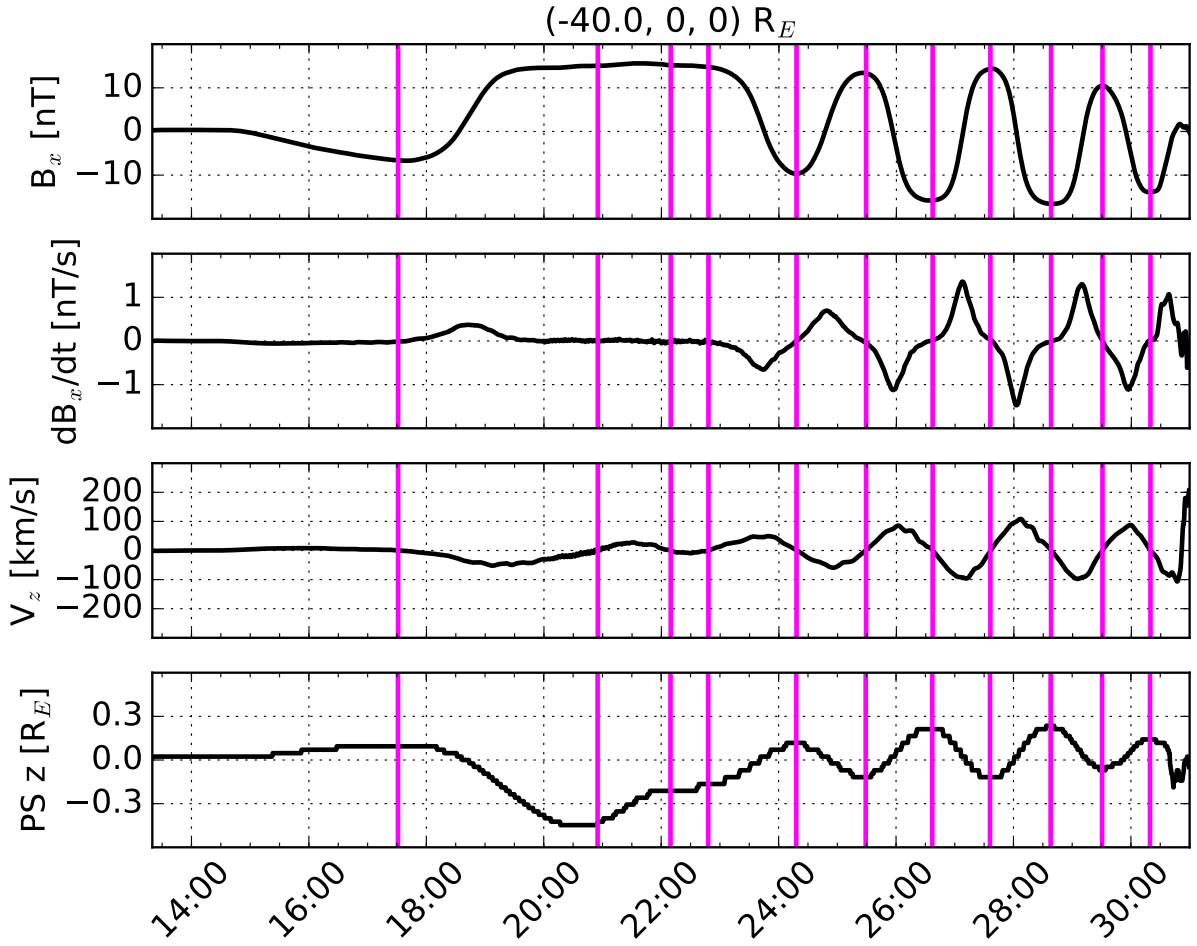

Figure 7. Time series observed by a virtual satellite located at $x = -40$ $\mathrm{R_E}$ and $y = z = 0$ in the simulation. From top to bottom, the parameters shown are: Earthward component of the magnetic field (B_x, cf. Fig. 2), time derivative of B_x ($\partial B_x/\partial t$, cf. Fig. 3), north component of the ion bulk flow (V_z, cf. Fig. 4), and location of the plasma sheet center in the z direction (PS z, cf. Fig. 5). The vertical magenta lines identify flapping half periods based on sign changes of V_z, and they correspond to the magenta dots at $x = -40$ $\mathrm{R_E}$ in Fig. 4.

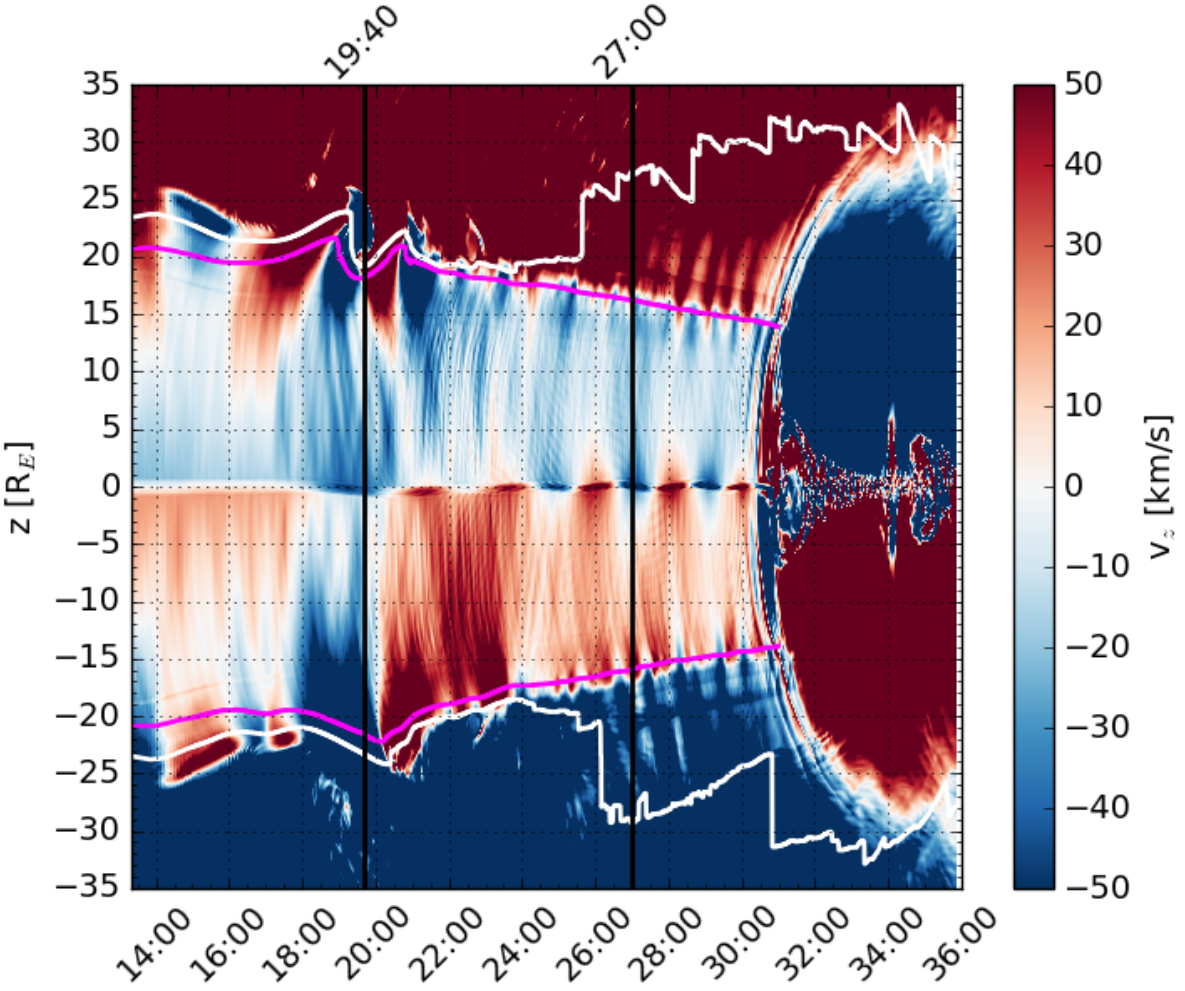

Figure 8. North component of the ion bulk velocity (V_z) as a function of z and time at $y = 0$ and $x = -40$ $\mathrm{R_E}$. The vertical black lines are the same as in Fig. 2. The white and magenta (only plotted until 31:00) curves indicate the innermost boundaries where $\beta_\perp > 1$ and $\beta_\perp > 0.1$ in the region $|z| > 5$ $\mathrm{R_E}$, respectively. The tail lobes are estimated to lie between the white curves and the magnetosonic wave resonance cavity between the magenta curves.

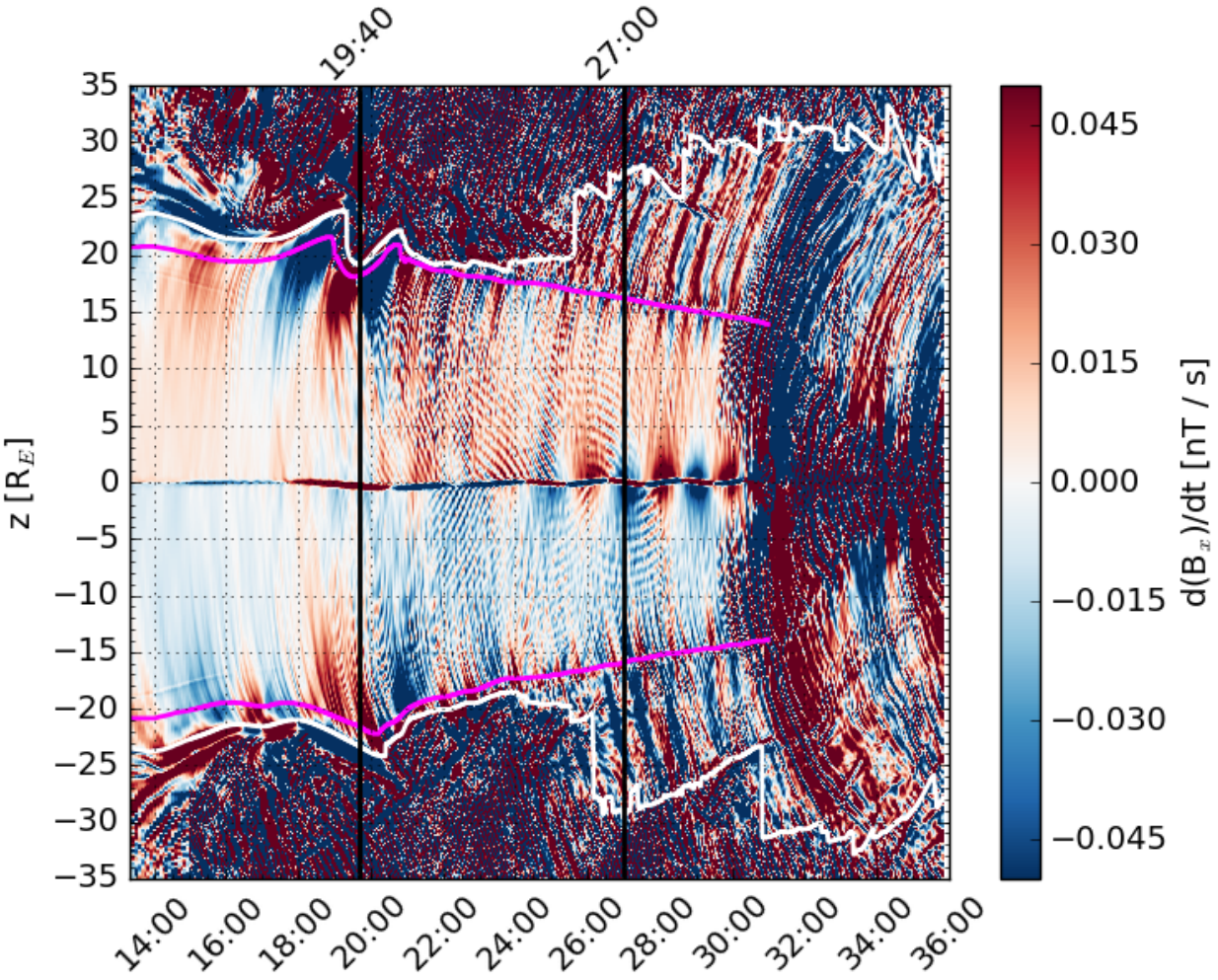

Figure 9. The same Fig. 8 except that the color shows the time derivative of B_x.

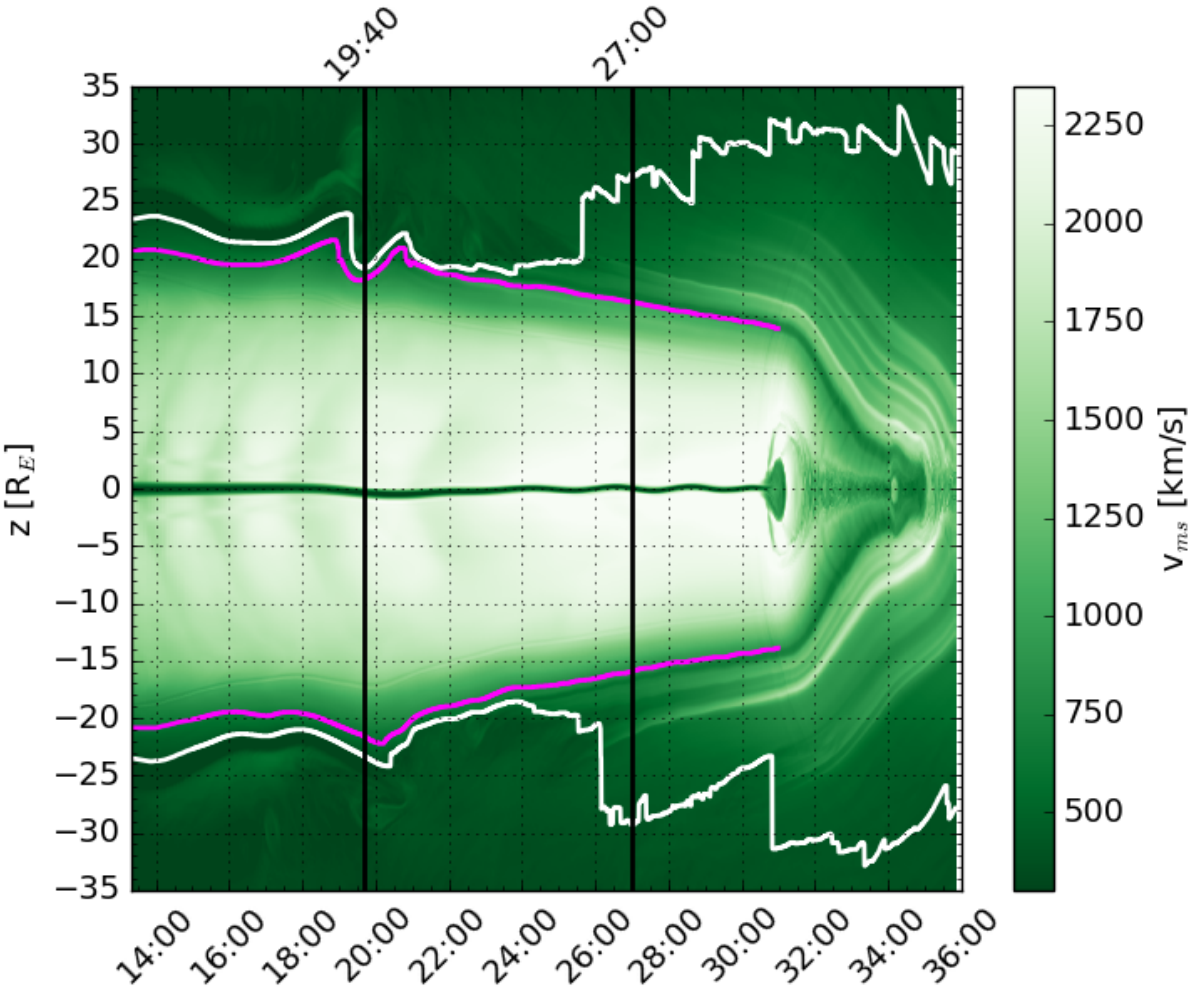

Figure 10. The same Fig. 8 except that the color shows the magnetosonic speed (V_{ms}).

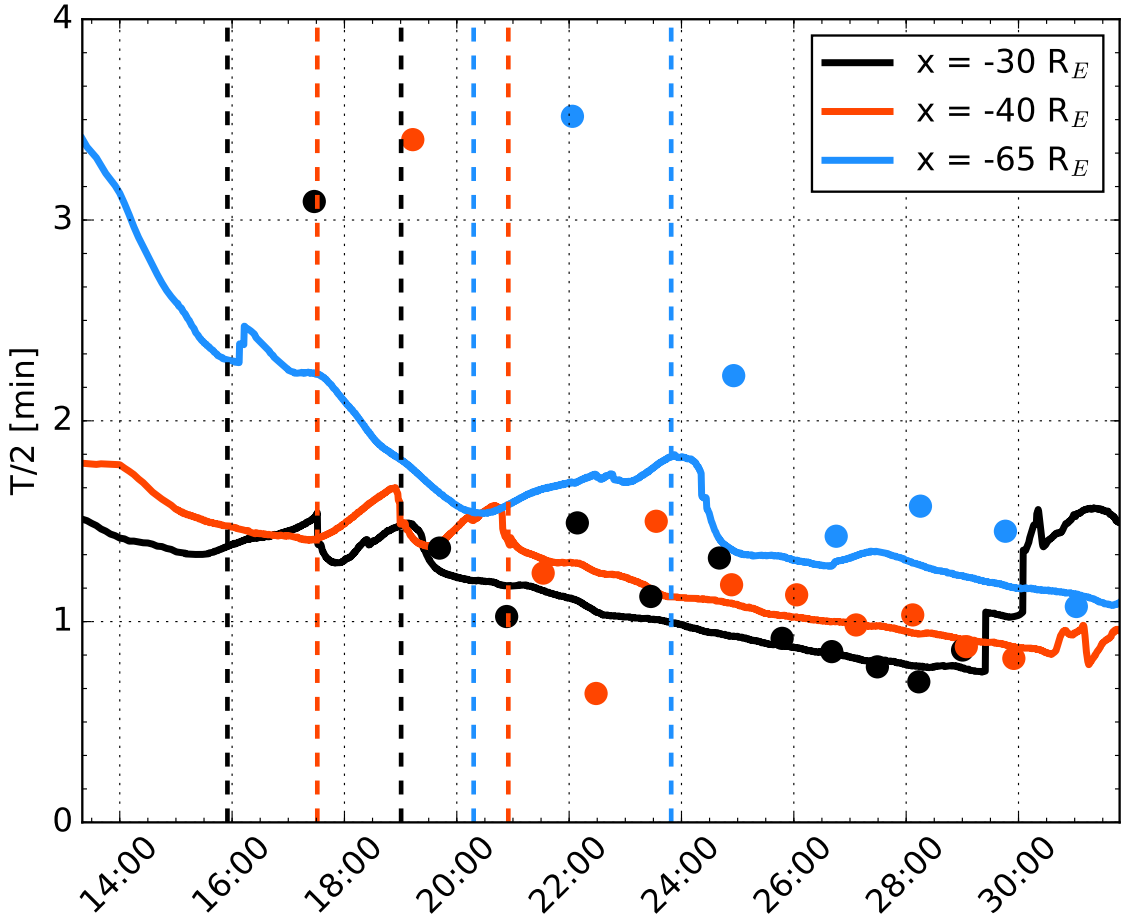

Figure 11. Travel time of magnetosonic waves across half of the magnetotail resonance cavity ($T/2$) at distances $x = -30$ $\mathrm{R_E}$ (black), $x = -40$ $\mathrm{R_E}$ (red), and $x = -65$ $\mathrm{R_E}$ (blue) as a function of time (solid curves). For example, $T/2$ at $x = -40$ $\mathrm{R_E}$ has been estimated by integrating $dt = dz/V_{ms}$ over the distance between the magenta curves marked in Fig. 10 and dividing by 2. The dots indicate tail flapping half periods with color indicating the corresponding x-coordinate. The flapping half periods have been obtained as the time differences between consecutive magenta dots indicated in Fig. 4, and they have been associated with a time stamp corresponding to the average of the two times. The dashed vertical lines show the start and end time of the first flapping signature at the three distances.